

Hidden charm in the COMPASS experiment at CERN

Bárbara Lopes Pereira^{1,a}

¹Faculdade de Ciências da Universidade de Lisboa, Lisboa, Portugal

Project supervisor: Catarina Quintans

October 13, 2023

Abstract. This work focuses on the study of the two $c\bar{c}$ vector-mesons, J/ψ and $\psi(2S)$, so-called charmonium resonances, that decay to two opposite charged muons. The study is based on the data collected in 2018 by the COMPASS experiment at CERN. The selection of events is optimized, to keep only primary vertices located at the nominal target regions and with good quality outgoing muon pairs. The dimuons mass spectrum is fitted in order to obtain the best signal to background ratio in the regions dominated by the J/ψ and $\psi(2S)$ resonances. We attempt to characterize the J/ψ and $\psi(2S)$ from the dimuon kinematic distributions in their respective dominant mass regions.

KEYWORDS: COMPASS, $J/\psi, \psi(2S)$, BACKGROUND

1 Introduction

1.1 COMPASS Experiment

COMPASS (Common Muon and Proton Apparatus for Structure and Spectroscopy) is a fixed-target and high energy experiment at the M2 beam line of the SPS (Super Proton Synchrotron) at CERN devoted to the study of hadron structure and the spectroscopy of exotic and hybrid light mesons. In the 2018 data taking, the focus of the experiment was the measurement of the polarized Drell-Yan process. An almost pure 190 GeV pion beam interacts with a set of targets placed sequentially: two polarized cells of ammonia (NH_3) and two unpolarized cells of aluminium (Al) and tungsten (W), respectively. The antiquark \bar{u} from the pion may interact with a quark u from a nucleon in the target, originating in the final state a pair of oppositely-charged muons, $\mu^+\mu^-$.

In the typical (from COMPASS data taking in 2015) invariant mass spectrum of the dimuons originated from the ammonia target, we can observe two peaks, as it is shown in figure 2.

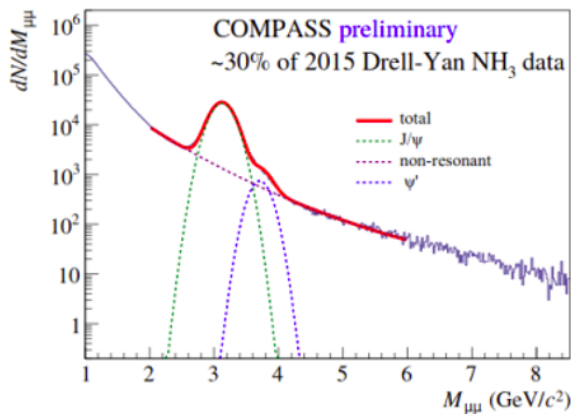


Figure 2. Dimuon invariant mass spectrum from the NH_3 target, obtained by the COMPASS experiment in 2015.

^ae-mail: fc56406@alunos.fc.ul

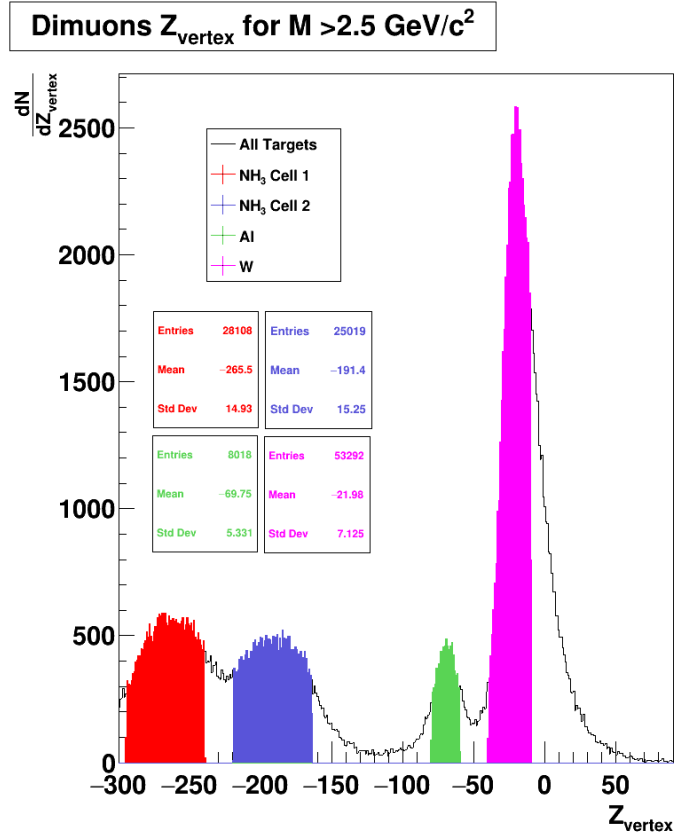


Figure 1. Distribution of dimuon events as a function of Z_{vertex} . The position of each COMPASS target is represented by a different color.

Each peak corresponds to a resonance, a very short-lived $c\bar{c}$ vector-meson, also known as charmonium. The first peak corresponds to the J/ψ particle with an invariant mass of $m = 3.097 GeV/c^2$ and the second peak is an excited state of charmonium, $\psi(2S)$, with invariant mass $m = 3.686 GeV/c^2$ [2].

The $\psi(2S)$ particle may decay either to J/ψ or directly to an opposite charged muon pair, being this the case for the events observed in the second peak. Charmonium particles are mainly produced by two different mechanisms: The first mechanism consists in the annihilation of a quark from the target and an anti-quark from the beam. The second mechanism consists in gluon-gluon fusion, with one gluon from the beam and the other gluon from the target. Both mechanisms are illustrated in figure 3.

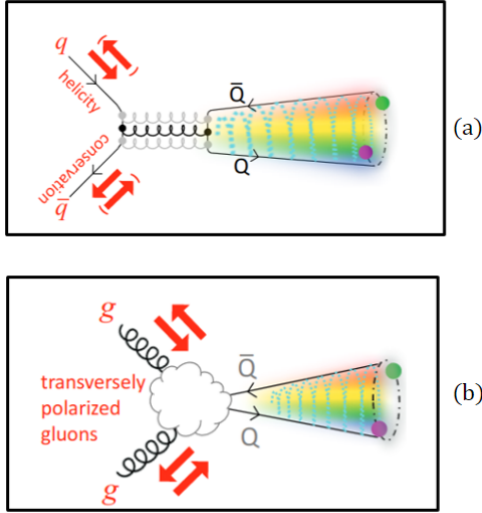


Figure 3. Illustrative scheme of the production mechanisms of J/ψ : (a) quark-antiquark annihilation; (b) gluon-gluon fusion. Image courtesy of P. Faccioli

1.2 COMPASS Experimental Setup

The setup has a two-staged spectrometer and several detectors of different types to identify the particles and reconstruct their trajectories. First we have the two polarized ammonia target cells followed by an hadron absorber, with the aluminium target and the heavy tungsten target inside it, in order to clean the muon sample required for the analysis, excluding hadrons from passing this stage in the apparatus. The spectrometer includes two muon walls made of iron and concrete in order to make sure the sample is made mainly of muons, since muons barely interact. After the muon walls there are hodoscopes, fast detectors made of plastic scintillator, used to trigger on interesting events. The spectrometer includes three trigger systems of two hodoscopes each:

- LAS system - consists on two large hodoscopes which are HG01 ($Z=585$ cm) and HG02 ($Z=1610$ cm) localized in the Large Angle Spectrometer (LAS);
- Outer system - consists on two hodoscopes which are HO03 ($Z=2150$ cm) and HO04 ($Z=3970$ cm) placed downstream in the Spectrometer, in the Small Angle Spectrometer (SAS);
- Middle system - consists on two small hodoscopes which are HM04 ($Z=4023$ cm) and HM05 ($Z=4784$ cm)

placed in the Small Angle Spectrometer (SAS) to cover part of the central dead region of the Outer system.

The trigger signals events to be saved by the Data Acquisition of COMPASS. The trigger information itself is stored as a trigger bit pattern. The trigger bit is associated with one of the hodoscope systems mentioned earlier. Two of the main dimuon triggers are:

- LAS-LAS: both opposite charged muons hitting LAS (identified as trigger bit 8);
- LAS-OT: one muon hitting the Outer System (SAS) and the other muon hitting the LAS (identified as trigger bit 4).

The COMPASS experimental setup is represented in figure 4.

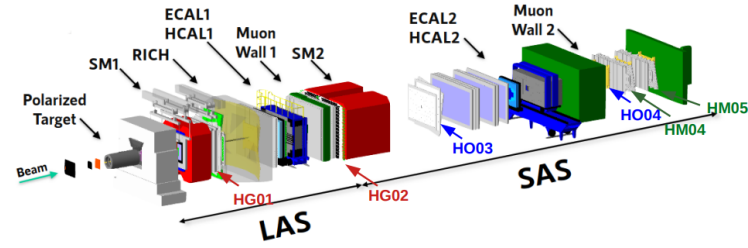


Figure 4. Illustrative scheme of the COMPASS experimental setup at CERN.

1.3 Kinematic Variables

In order to study the characteristics of J/ψ and $\psi(2S)$ and compare these two resonances, we consider the following kinematic variables: Feynman- x , x_F ; beam Bjorken- x , x_π ; target Bjorken- x , x_N ; and the transverse momentum of the opposite charged muon pair, P_T .

x_π represents the fraction of momentum of the anti-quark annihilating carried by the pion parent, while x_N represents the fraction of momentum of the quark annihilating carried by the nucleon parent. The Feynman- x , x_F , is calculated in the center of mass rest frame of the collision of the pion and beam hadrons, called Hadrons Collision Frame (HCF). We obtain the x_F value by considering the dimuons longitudinal momentum, $P_{Z_{\psi^*}}$, and the center-of-mass energy of the hadrons collision, \sqrt{s} , according to the following expression:

$$x_F = \frac{P_{Z_{\psi^*}}}{\sqrt{s}/2} |_{HCF} \quad (1)$$

The fractions of momentum x_π and x_N are calculated by considering the Feynman- x , x_F , and the invariant mass of the dimuons (equivalent to Q in Drell-Yan), as we can see in the following expressions:

$$x_\pi = \frac{\sqrt{x_F^2 + \frac{4Q^2}{s}} + x_F}{2} \quad (2)$$

$$x_N = \frac{\sqrt{x_F^2 + \frac{4Q^2}{s}} - x_F}{2} \quad (3)$$

The transverse momentum of the dimuons, P_T , corresponds to the dimuons momentum along the transverse direction of the beam and it can be obtained by the following expression:

$$P_T = \sqrt{P_X^2 + P_Y^2} \quad (4)$$

2 Event selection

We need to optimize the event selection in order to improve the resolution of the resonance peaks observed in the dimuons invariant mass spectrum.

First, we selected the events from 30 runs (approximately one and half days of data taking) collected by COMPASS in 2018, using the PHAST *software* [3], a data analysis package providing direct access to the properties of the reconstructed trajectories of the particles at any point, including the vertex of the interaction.

For each event, we choose the best quality vertex, according to space and time criteria. We select the events in which the final state particles correspond to two opposite charge muons, which means selecting one particle with PID=5 and another particle from the same vertex with PID=6, making sure that the muon pair is confirmed to fire one of the dimuon triggers. The trigger is validated by checking that each muon track effectively crossed the trigger system that fired. For example, if the LAS-OT trigger fired (trigger bit 4), we verify that one of the muon tracks, extrapolated to the HG01 and HG02 positions, is within the active area of these hodoscopes, while the other muon track is extrapolated to positions of HO03 and HO04 in order to confirm that the track is within the active area of these other hodoscopes (referred as *trigvalOTLAS* == 1). If the LAS-LAS system fires, we extrapolate both muon tracks to the positions of HG01 and HG02 and verify if both muon tracks are within the active area of these hodoscopes (referred as *trigval2LAS* == 1).

We ensure the selection of good events that allow to study the physical properties of J/ψ and $\psi(2S)$, by applying the following quality cuts:

Table 1. Criteria for event selection.

Variable	Condition
Mean Time of Positive Muon, t_+	<1000 ns
Mean Time of Negative Muon, t_-	<1000 ns
$ t_+ - t_- $	< 3 ns
tracks χ^2/NDF	< 8
ZLAST	>1500 cm
ZFIRST	< 300 cm
$\chi_{vertex}^2 + Y_{vertex}^2$	< 4 cm^2
Trigger bit and Validation	(2 and trigvalOTLAS=1) or (8 and trigval2LAS ==1)
NH ₃ Cell 1	-294.5 < Z_{vertex} < -239.5 cm
NH ₃ Cell 2	-219.1 < Z_{vertex} < -163.9 cm
Al	-73.6 < Z_{vertex} < -66.5 cm
W	-30 < Z_{vertex} < -10 cm

After the application of the quality cuts to the data, as listed in table-1, we proceed to represent the invariant mass spectrum of the selected dimuons from each of the targets, as shown in figure 5: From the figure 5, we can see that the target in which the J/ψ resonance has the best mass resolution is in the first NH₃ target cell, which means the width

Dimuon Invariant Mass Spectrum

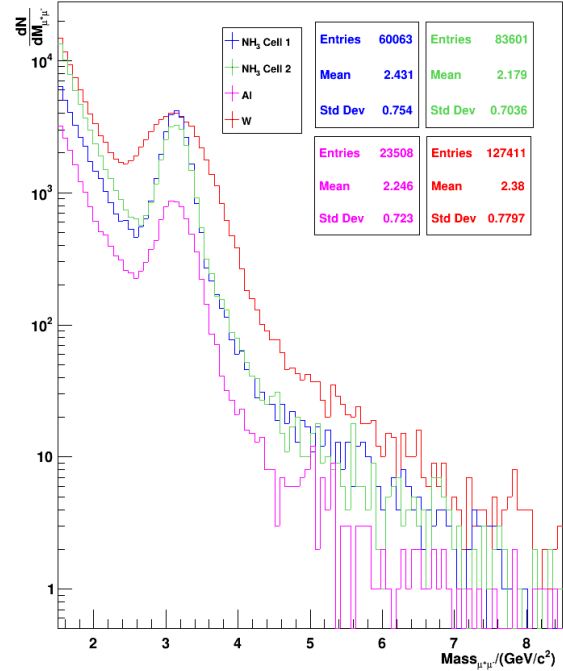


Figure 5. Invariant mass distribution of the dimuons selected per target.

of the J/ψ peak in the dimuon mass spectrum, for the first ammonia target is the smallest, while the mean mass value doesn't deviate much from the PDG listed value (nor in the other targets). So we will limit our analysis to the events selected from the first ammonia target, imposing the following condition to the position of the dimuon vertex along the z-axis : $-294.5 < Z_{vertex} < -239.5$ cm.

3 Results and Conclusions

3.1 Invariant mass spectrum of the dimuons

We will perform an effective fit to the invariant mass spectrum of the dimuons selected from the first ammonia target cell, in order to select the mass intervals in which each resonance, either J/ψ or $\psi(2S)$, are dominant.

The effective fit performed considers the peak of J/ψ , the peak of $\psi(2S)$ and other processes that may result in two muons in the final state such as Drell-Yan, open-charm semi-leptonic decays, and combinatorial random pairs, which we will designate by background.

To fit both peaks of J/ψ and $\psi(2S)$, we consider two normalized Gaussian distributions in which, according to the PDG, [2], the mean value of the $\psi(2S)$ must be distanced from the mean value of J/ψ by a value of $0.589 GeV/c^2$. The background is easily fitted by a negative power law function.

The final fit function to the invariant mass spectrum is given by the following expression:

$$\frac{dN}{dM_{\mu^+\mu^-}}(x) = N_{J/\psi} \frac{e^{-\frac{(x-\mu)^2}{2\sigma^2_{J/\psi}}}}{\sqrt{2\pi\sigma^2_{J/\psi}}} + N_{\psi(2S)} \frac{e^{-\frac{(x-\mu-0.589)^2}{2\sigma^2_{\psi(2S)}}}}{\sqrt{2\pi\sigma^2_{\psi(2S)}}} + ax^{-b} \quad (5)$$

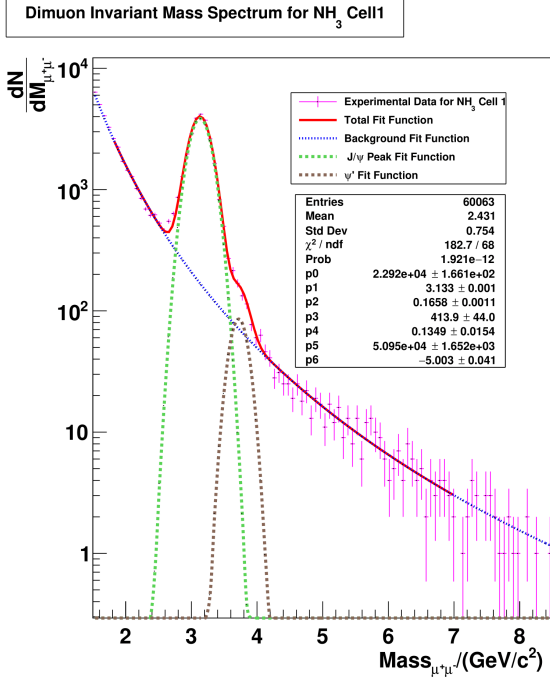


Figure 6. Fit to the invariant mass of the dimuons selected in the ammonia target.

From the figure 6, we can observe clearly the peak of J/ψ and the peak of $\psi(2S)$. The fit is used to identify the invariant mass intervals in which each resonance has the maximum signal to background ratio. We have determined, based on the data of the first ammonia target, that in the interval $[2.9\text{GeV}/c^2; 3.53\text{GeV}/c^2]$ the J/ψ to total is dominant, obtaining a J/ψ signal fraction of 93.74%. From the peak of the normalized Gaussian in the fit we estimate a total number of 22919 J/ψ particles originated in the ammonia first cell.

Then we proceed to get the interval in which we get the maximal ratio of $\psi(2S)$ to background. In the interval of $[3.6\text{GeV}/c^2; 3.95\text{GeV}/c^2]$, we get a $\psi(2S)$ ratio of 45.02%, including in the background a contamination from the J/ψ tail of 7.81%. We cannot reliably estimate the number of $\psi(2S)$ particles, given the fact that the relative uncertainty related to its normalization parameter in the fit (p3) is above 10%. Even though, it was already remarked that the J/ψ peak had a better resolution for the first ammonia target, the dimuon mass spectra with only the data selected by the quality criteria stated in Table 1 of the rest of the targets (NH_3 Cell 2; Al ; W) were fitted by a fit function. Both dimuon mass spectrum of the targets NH_3 Cell 2 and Al were fitted by the equation 5. The tungsten target (W) was fitted with the same Gaussian distributions expressed

in the 5, however the background was described by the combination of a power law and a decaying exponential, as we can state in the equation 6:

$$\frac{dN}{dM_{\mu^+\mu^-}}(x) = N_{J/\psi} \frac{e^{-\frac{(x-\mu)^2}{2\sigma^2_{J/\psi}}}}{\sqrt{2\pi\sigma^2_{J/\psi}}} + N_{\psi(2S)} \frac{e^{-\frac{(x-\mu-0.589)^2}{2\sigma^2_{\psi(2S)}}}}{\sqrt{2\pi\sigma^2_{\psi(2S)}}} + ax^{-b} + ce^{-dx} \quad (6)$$

The results on the fits performed to the dimuon mass spectra from each target are displayed in table 2.

From the results of the effective fits performed for each of the targets we can confirm that the J/ψ peak has a better resolution in the data from the first ammonia target and we can still verify the $\psi(2S)$ resonance has a better resolution in both ammonia targets in comparison to the tungsten and aluminium targets.

3.2 J/ψ and $\psi(2S)$ region kinematic distributions

After the effective fits to the mass spectra we determine the intervals in which we get the highest signal fraction for each resonance. We then study the kinematic distributions in terms of x_F , x_π , x_N and P_t variables, for the events in each of these mass intervals.

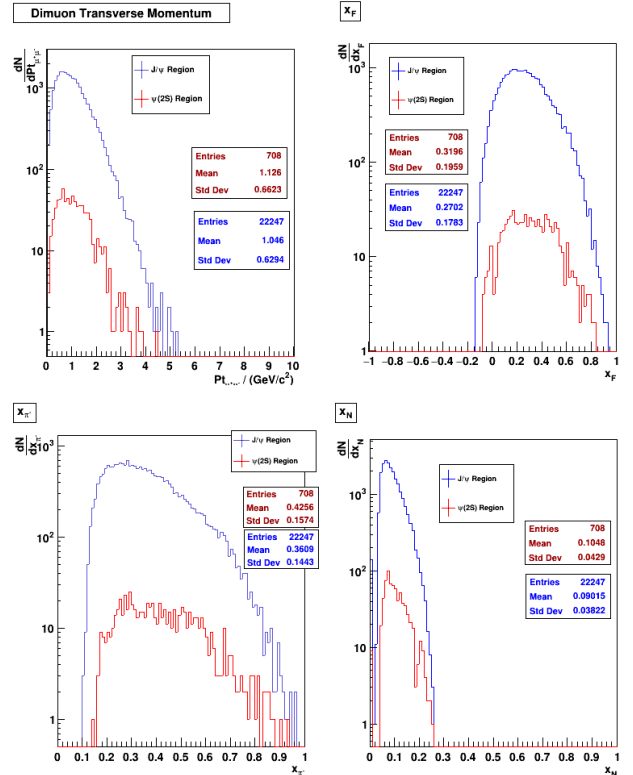


Figure 7. Kinematic distributions for J/ψ region and $\psi(2S)$ region, identified from the data of the first ammonia target.

From figure 7, we can conclude that the resonance regions identified have characteristics that distinguish them. However, we cannot conclude based on these.

In the interval of mass where we identified the highest percentage of $\psi(2S)$, obtaining a $\psi(2S)$ fraction of

Table 2. Fit results for all the target cells.

	NH3 Cell 1	NH3 Cell 2	Al cell	W cell
$\mu/(GeV/c^2)$	3.133	3.138	3.123	3.111
$\sigma_{J/\psi}/(GeV/c^2)$	0.166	0.176	0.218	0.325
$\sigma_{\psi(2S)}/(GeV/c^2)$	0.135	0.193	0.202	0.305
Number of J/ψ particles	22919	19131	6137	42861
$M_{\mu^+\mu^-}$ range $/(GeV/c^2)$	[2.9; 3.53]	[2.9; 3.53]	[2.76; 3.53]	[2.55; 3.6]
$J/\psi/Total(\%)$	93.60	91.32	87.88	83.65
$\psi(2S)/Total(\%)$	0.14	0.50	0.23	1.80
$M_{\mu^+\mu^-}$ range $/(GeV/c^2)$	[3.6; 3.95]	[3.6; 3.95]	[3.6; 3.88]	[3.67; 3.95]
$\psi(2S)/Total(\%)$	45.02	48.74	17.97	24.11
$J/\psi/Total(\%)$	7.81	10.36	37.47	57.46

45.02%, there is still the contribution of J/ψ and other background of 54.98%, which is too large to be neglected.

Acknowledgements

I would like to thank Catarina Quintans for the guidance, availability and enthusiastic approach of the project, which allowed me to have the most profitable experience to my

academic future and deeply motivated my interests in Particle Physics.

References

- [1] *COMPASS*; <http://wwwcompass.cern.ch/>, (2023).
- [2] Particle Data Group (PDG); https://pdg.lbl.gov/2023/html/computer_read.html, (2023).
- [3] *Phast*; <https://ges.web.cern.ch/ges/phast/index.html>